Tailored SU-8 micropillars superhydrophobic surfaces enhance conformational changes in breast cancer biomarkers

Angelo Accardo, Emmanuelle Trévisiol, Aline Cerf, Christophe Thibault, Henrik Laurell, Melissa Buscato, Françoise Lenfant, Coralie Fontaine, Christophe Vieu

Tailored SU-8 micropillars superhydrophobic surfaces enhance conformational changes in breast cancer biomarkers

Running title: SU8 Micro-pillars enhance structure differences in ERα biomarkers

Running Authors: Accardo et al.

Angelo Accardo[a)]

INSERM U1048-I2MC-CHU Rangueil, BP 84225, 31432 Toulouse, Cedex 4, France

LAAS-CNRS, Université de Toulouse, CNRS, Toulouse, France

Emmanuelle Trevisiol

LAAS-CNRS, Université de Toulouse, CNRS, Toulouse, France

Aline Cerf

LAAS-CNRS, Université de Toulouse, CNRS, Toulouse, France

Christophe Thibault

LAAS-CNRS, Université de Toulouse, CNRS, INSA, Toulouse, France

Henrik Laurell

INSERM U1048-I2MC-CHU Rangueil, BP 84225, 31432 Toulouse, Cedex 4, France

Melissa Buscato

INSERM U1048-I2MC-CHU Rangueil, BP 84225, 31432 Toulouse, Cedex 4, France

Françoise Lenfant

INSERM U1048-I2MC-CHU Rangueil, BP 84225, 31432 Toulouse, Cedex 4, France

Jean-Francois Arnal

INSERM U1048-I2MC-CHU Rangueil, BP 84225, 31432 Toulouse, Cedex 4, France

Coralie Fontaine

INSERM U1048-I2MC-CHU Rangueil, BP 84225, 31432 Toulouse, Cedex 4, France

Christophe Vieu

LAAS-CNRS, Université de Toulouse, CNRS, INSA, Toulouse, France

[a)] Electronic mail: aaccardo@laas.fr , angelo.accardo@inserm.fr

Here we report the fabrication of lotus-leaves-like tailored SU8 micropillars and their application in the context of a multi-technique characterization protocol for the investigation of the structural properties of the two estrogen receptors (ERα66/ERα46). ER (α) expression is undoubtedly the most important biomarker in breast cancer, because it provides the index for sensitivity to endocrine treatment. Beside the well-characterized ERα66 isoform, a shorter one (ERα46) was reported to be expressed in breast cancer cell line. The superhydrophobic supports were developed by using a double step approach including an optical lithography process and a plasma reactive ion roughening one. Upon drying on the micropillars, the bio-samples resulted in stretched fibers of different diameters which were then characterized by synchrotron X-ray diffraction (XRD), Raman and FTIR spectroscopy. The evidence of both different spectroscopic vibrational responses and XRD signatures in the two estrogen receptors suggests the presence of conformational changes between the two biomarkers. The SU8 micropillar platform therefore represents a valid tool to enhance the discrimination sensitivity of structural features of this class of biocompunds by exploiting a multi-technique *in-situ* characterization approach.

I. INTRODUCTION

The use of microfluidic engineered devices for tuning the conformation and arrangement of biomedical compounds[1-3] is widely extended in the nanobiotechnlogy community. From one side, the use of droplet-based digital microfluidics architectures triggers the interest of the scientific community in the biological and chemical fields, due to the possibility of controlling complex processes by means of a programmable sequence

of discrete steps and with volumes sensitively smaller than those used in continuous flow microfluidics[4-6]. On the other hand, dedicated lab on a chip devices in combination with advanced characterization techniques (e.g. Raman/FTIR spectroscopy and X-ray diffraction) allow to extrapolate sensitive structural information on biomedical relevant subjects[7-10]. In this work we propose the fabrication of lotus-leaves-like tailored surfaces, following a biomimetic approach inspired by natural Lotus Leaves[11], as a tool to enhance the formation of free-standing fibers coming from two Estrogen Receptors (ER) isoforms namely ERα46 and ERα66. Estrogen receptor α (ERα), is holding a key position in the diagnosis of breast tumors in several aspects[12]. ERα protein immunoreactivity in the nucleus of mammary epithelial cells is systematically evaluated and quantified during the anatomopathologic diagnosis, and 70% of breast cancers are initially described as ERα positive[12]. ERα can be divided in 6 domains from A to F and in addition to the full length 66kDa (ERα66), a 46kDa ERα-isoform (ERα46), lacking the N-terminal portion (domains A/B) can be expressed through either an alternative splicing[13] or an internal entry site[14]. ERα46 has been reported in breast cancer cell lines where it inhibits the proliferative response to estrogen mediated by ERα66 in the MCF7 breast cancer cell line[15]. However, all studies conducted on breast cancer diagnosis focused on the full length isoform ERα66, and very little information is available about the expression of ERα46 in breast tumors probably due to the absence of a reliable tool to study ERα46. From a structural point of view, the absence of the flexible A/B domain in ERα46[16] should translate in a different vibrational mode. In order to support this hypothesis, we combined the use of biomimetic superhydrophobic surfaces to Raman, FTIR and synchrotron X-ray microdiffraction. The Raman and FTIR Amide I/III bands[9] can indeed

provide sensitive information on the structural variations of the analyzed sample while, by using a synchrotron source X-ray microbeam, it is possible to detect different small- and wide-angle X-ray scattering (SAXS/WAXS) signatures[10,17] linked to the conformation of the solid residues formed upon evaporation. By exploiting the peculiar microfluidic flows provided by droplets in a superhydrophobic state and their highly homogeneous evaporation rate[17] it was indeed possible to obtain well aligned fiber structures which highlighted in the two estrogen receptors ERα46 and ERα66 different secondary structure conformations (in terms of α-helical and β-sheet composition) making this platform a useful tool for further characterization of this class of biomarkers.

II. EXPERIMENTAL

A. Fabrication of the SU8 micropillars supports

SU8 micropillars were developed by exploiting a double step approach involving optical lithography and plasma reactive ion roughening. The microstructures were grown either on CaF_2 windows (Crystran, for Raman and FTIR measurements) or on 5mm X 5mm square Si_3N_4 membranes (for XRD measurements).

The Si_3N_4 membranes were fabricated exploiting the following protocol: selection a <100> wafer Si_3N_4 – Si – Si_3N_4 with a nitride thickness of 500 nm on both sides; spin coating of S1813 positive tone resist (Microchem®) on the wafer at 4000 rpm for 60 s and baking at 90°C for 3 minutes; soft contact exposure for 15 seconds and development with MF-319 developer for 1 minute for removing the resist from the square areas; rinse in water and baking of the wafer for 1 minute to dry it completely; plasma reactive ion etching using CHF_3 (sccm 70) and O_2 (sccm 5), RF power =70 W, Source power =

200W, P = 1Pa; resist stripping with Acetone (cold, 3 min); KOH wet etch (100 g of KOH (Sigma®) in 150 ml of H_2O, 105°C) and final rinse of the wafer in milliQ water.

The SU8 circular micropillars (arranged in a hexagonal lattice with 10 μm diameter, 20 μm inter-pillar gap and 20 μm height) were fabricated using the following protocol: spin-coating of SU8-25 resist (Microchem®) at 1500 rpm for 60 s; prebake at 65°C for 5 min followed by 40 min at 95°C; hard contact exposure for 4.5 s; post-bake at 65°C for 5 min followed by 10 min at 95°C; development in SU8 developer for 9 min and rinse in IPA for 1 min; plasma reactive ion roughening (Trikon-SPTS) of the pillars head using CF_4 (5 sccm), O_2 (15 sccm), P = 9.06 Pa, RF power = 50 W, Source power = 100 W; Teflon deposition by plasma process using C_4F_8 (75 sccm), P = 3.6 Pa, Source power = 600 W, RF power = 1 W.

B. Configuration of the Raman, FTIR and Synchrotron beamline setup.

Raman measurement were performed with a Horiba Labram Raman setup, using a 632 nm laser line with a laser beam of 2 μm X 2μm spotsize, 6 s of exposure, 1% of laser intensity and 10 accumulations. FTIR characterizations have been performed in transmission with a Bruker FTIR microscope exploiting a Globar Source in the Mid-infrared range, an MCT detector and a spot-size of 10X10 μm^2. OMNIC software has been employed for the interpretation of the spectral data. Synchrotron X-ray diffraction (XRD) experiments were performed at the ID13 beamline of the European Synchrotron Radiation Facility in Grenoble. The wavelength of the monochromatic X-ray beam was equal to 0.935735 Å (E=12.99986 KeV) with a beam spot dimension of 2.3 μm (ver) X

2.5 μm (hor) and a sample to detector distance of 185,047 mm calibrated with Al_2O_3 calibrant. Regions of interest of the sample were selected using an onaxis optical Olympus microscope aligned with the focal spot of the microbeam. The expression of the scattering vector Q in the illustrated azimuthal averages is equal to $Q = 4\pi \sin\theta/\lambda$, where θ is the diffraction angle and λ is the X-ray wavelength. FIT2D software has been used for data analysis of the XRD patterns.

C. Preparation of the Estrogen receptor samples

The cDNA coding for ERα66 and ERα46 protein was cloned .I*n vitro* expression of ERα66 and ERα46was performed by using *in vitro* transcription and translation (TNT)-coupled rabbit reticulocyte extracts according to manufacturer's recommended conditions (Promega). The obtained samples were afterwards incubated at 30°C for 90 min and water transferred by centrifuging them 5 times at 13 KRPM for 5 min using Vivaspin 500 columns (Sartorius Stedim) equipped with 30000 Da MWCO (molecular weight cut off) filters. Samples were then stored at -80°C before deposition on the micropillared supports.

D. SEM investigation and contact angle setup

SEM imaging was performed on the samples metal-coated with 15 nm of sputtered gold by using a Hitachi S-4800 setup with a 5 kV acceleration voltage. Contact angle measurement were acquired using a Digidrop system (GBX) and the imaging software Image J.

III. RESULTS AND DISCUSSION

A. Morphological investigation and FTIR characterization of the ER samples dried on SU8 micropillars

Droplet of 5 µL volume, containing either ERα46 or ERα66, were deposited on top of the SU8 micropillars (Figure 1A,B) reaching a contact angle of 158°. This superhydrophobic behaviour was reached thanks to the combination of a well-defined topology, achieved by the optical lithography step and plasma roughening, with a Teflon layer, obtained by plasma deposition of C_4F_8, whose intrinsic contact angle is of 114°.

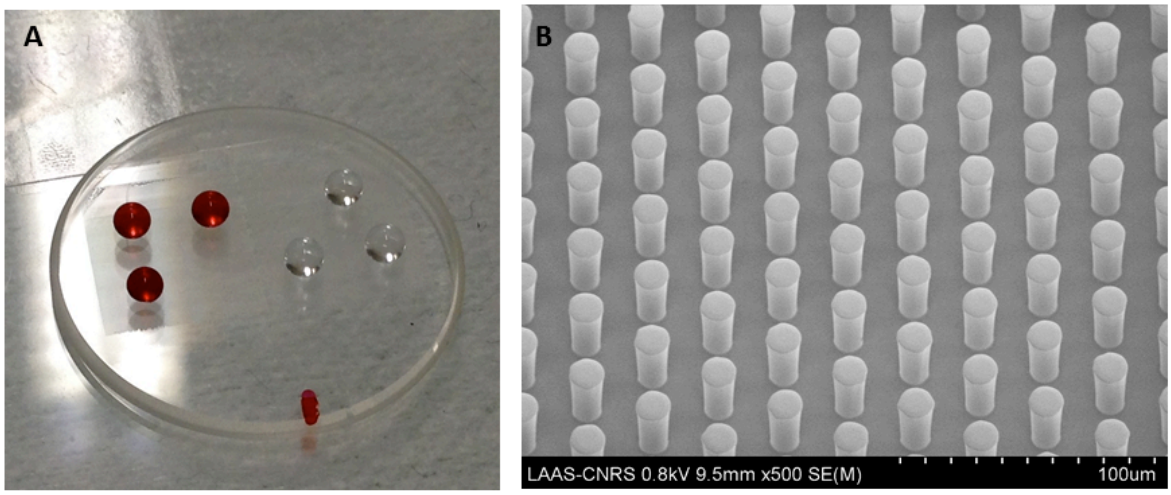

FIG. 1. A: Droplets of ERα solutions and MilliQ water sitting on a SU8 micropillared surface fabricated on top of a CaF_2 window; B: SEM micrograph of the SU8 micropillar morphology.

The complete evaporation of the solution droplets was reached after 1h. Upon drying, it was possible to observe the formation of free standing fiber structures of different diameters suspended between the SU8 pillars (Figure 2).

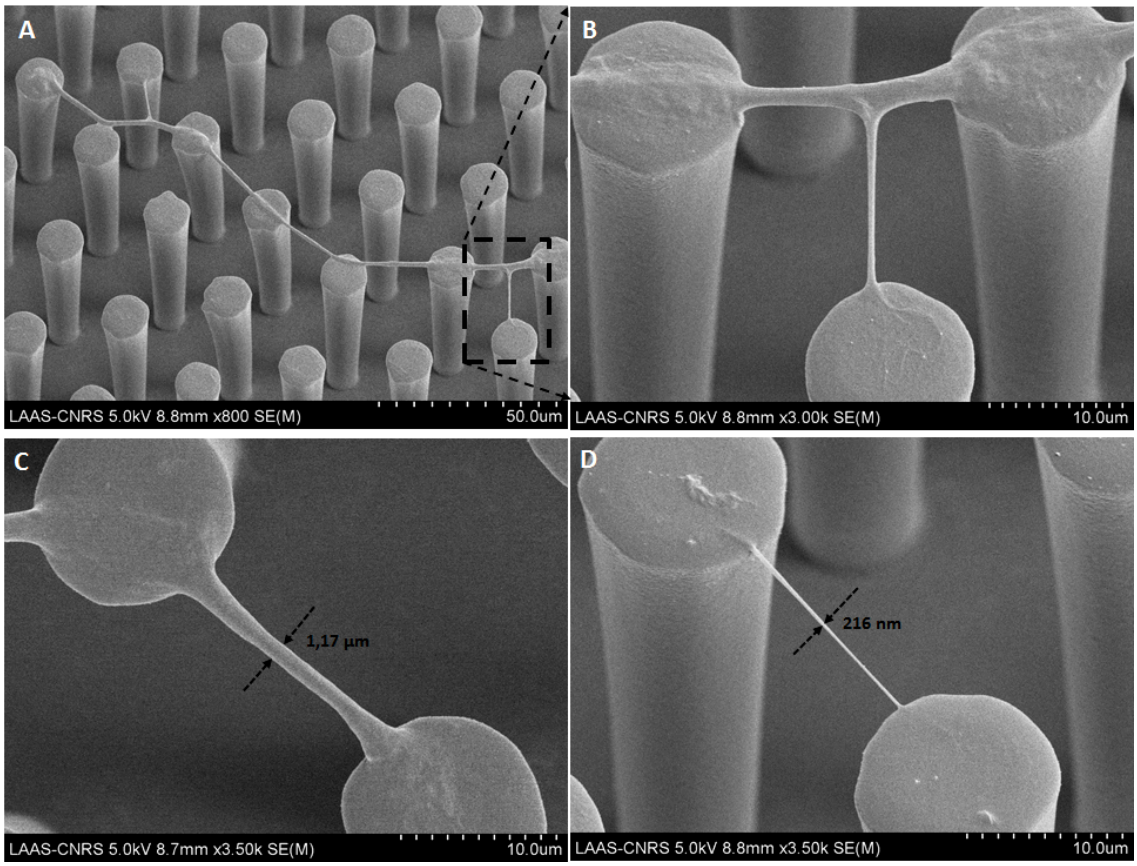

FIG. 2. SEM micrographs of ERα fiber structures suspended between SU8 micropillars obtained upon drying.

We attribute the formation of such fibers to the stretching mechanism provided by the shrinking of the contact line of the droplet while drying and jumping from one pillar to the adjacent one.

Since the Amide I band is sensitive to protein secondary structure, FTIR spectroscopy is frequently used to study the process of protein misfolding and aggregation *in vitro*[18]. Due to unique hydrogen bonding environments for the different secondary structure elements, shifts are observed in the frequency of the Amide I band and it is possible to detect several features of protein secondary structure which allows discriminating among beta-

turn (1665-1685 cm^{-1}), alpha-helix (≈1655 cm^{-1}), unordered (≈1640 cm^{-1}) and beta sheet structures (1610–1640 cm^{-1})[19].

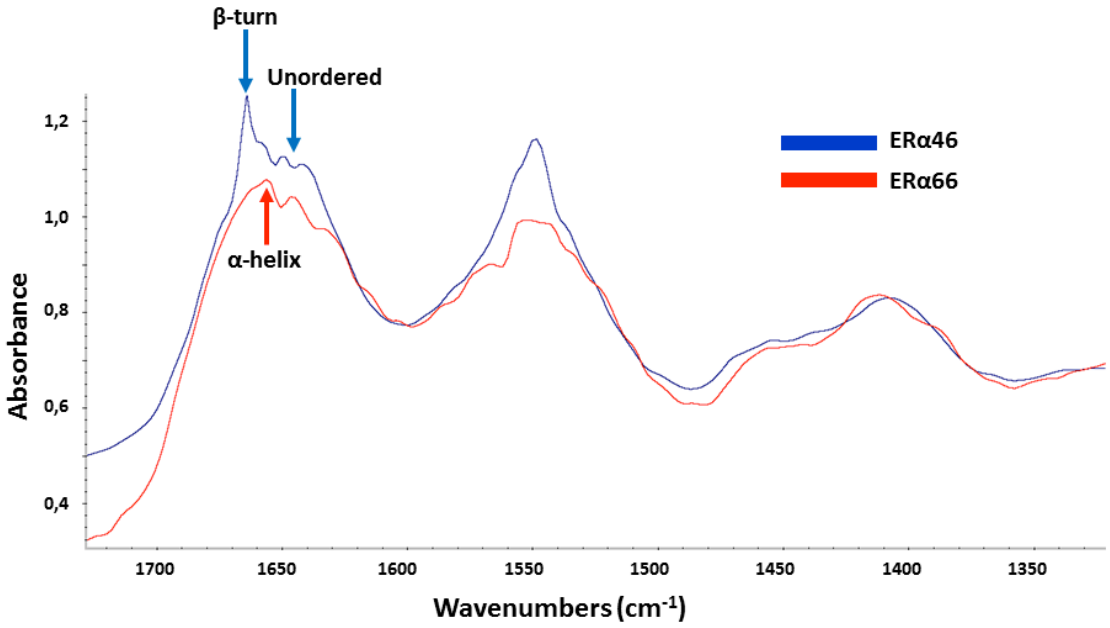

FIG. 3. FTIR spectra of the ERα46 and ERα66 samples dried on superhydrophobic SU8 micropillars.

The FTIR characterization of the two estrogen receptor samples dried on top of SU8 micropillars sitting on top of CaF_2 windows show how ERα46 and ERα66 seem to feature different molecular configurations as depicted in Figure 3. In particular, ERα46 has a main peak in the Amide I band at 1663 cm^{-1} (related to β-turn configuration) and two weaker contributions at 1649 and 1641 cm^{-1} (related to unordered phases). ERα66 on the other hand does not present the strong peak at 1663 cm^{-1} but, instead, a main contribution at 1656 cm^{-1} (related to α-helical phases). As a first hypothesis, this different secondary structure conformation could be ascribed by the absence of the flexible A/B domain in ERα46[16] which should translate in a different vibrational mode.

B. *Micro-Raman characterization of the ER samples dried on SU8 micropillars.*

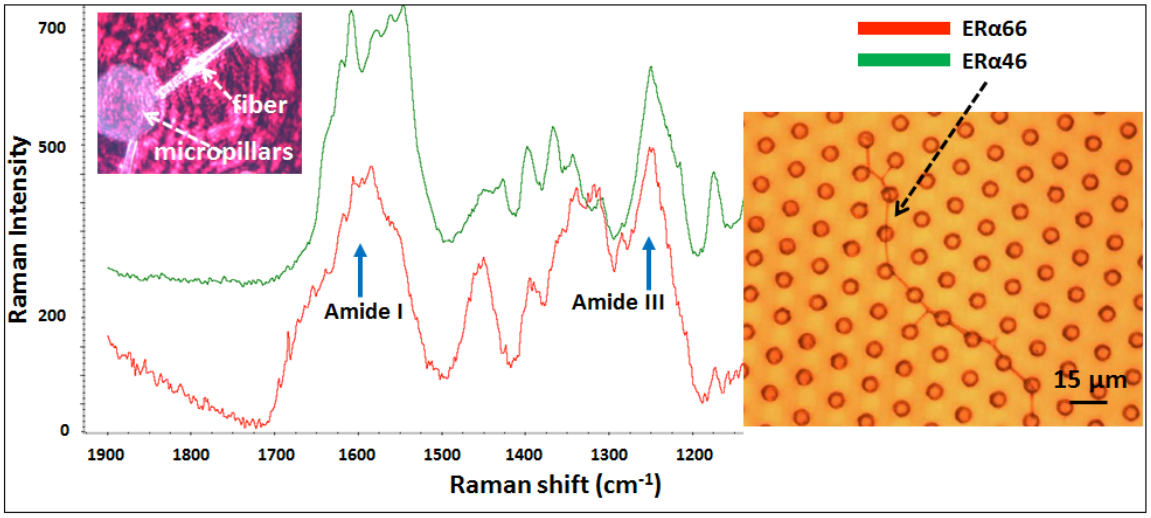

FIG. 4. Micro-Raman spectra of the ERα46 and ERα66 samples dried on superhydrophobic SU8 micropillars (inset: laser beam impinging the ER fiber and optical micrograph of the suspended fiber).

In support of the results obtained by FTIR measurements, we performed a parallel micro-Raman spectroscopy investigation as also with this characterization technique conformational information can be obtained by analyzing the amide I and amide III bands[20]. ERα46 sample evidenced a strong Amide III contribution at 1250 cm^{-1} (related to random coils and turns) and some weaker β-sheet components in the band 1229-1235 cm^{-1} while the Amide I band shows antiparallel β-sheets (1621 cm^{-1} and 1611 cm^{-1}) together with a weaker shoulder related to unordered phase (1640 cm^{-1}). On the other hand, compared to ERα46, ERα66 shows some structural differences in both the Amide I and Amide III bands. In particular, in the Amide III band, we could detect the co-presence of a random coils/turns peak at 1250 cm^{-1} and of a α-helical one[21] at 1282 cm^{-1}. In the Amide I band the strong antiparallel β-sheet peak at 1611 cm^{-1} disappeared while

the weaker component at 1621 cm^{-1} can still be detected together with a α-helical contribution at ≈1655 cm^{-1}.

C. *Synchrotron X-ray diffraction characterization of the ER samples dried on SU8 micropillars.*

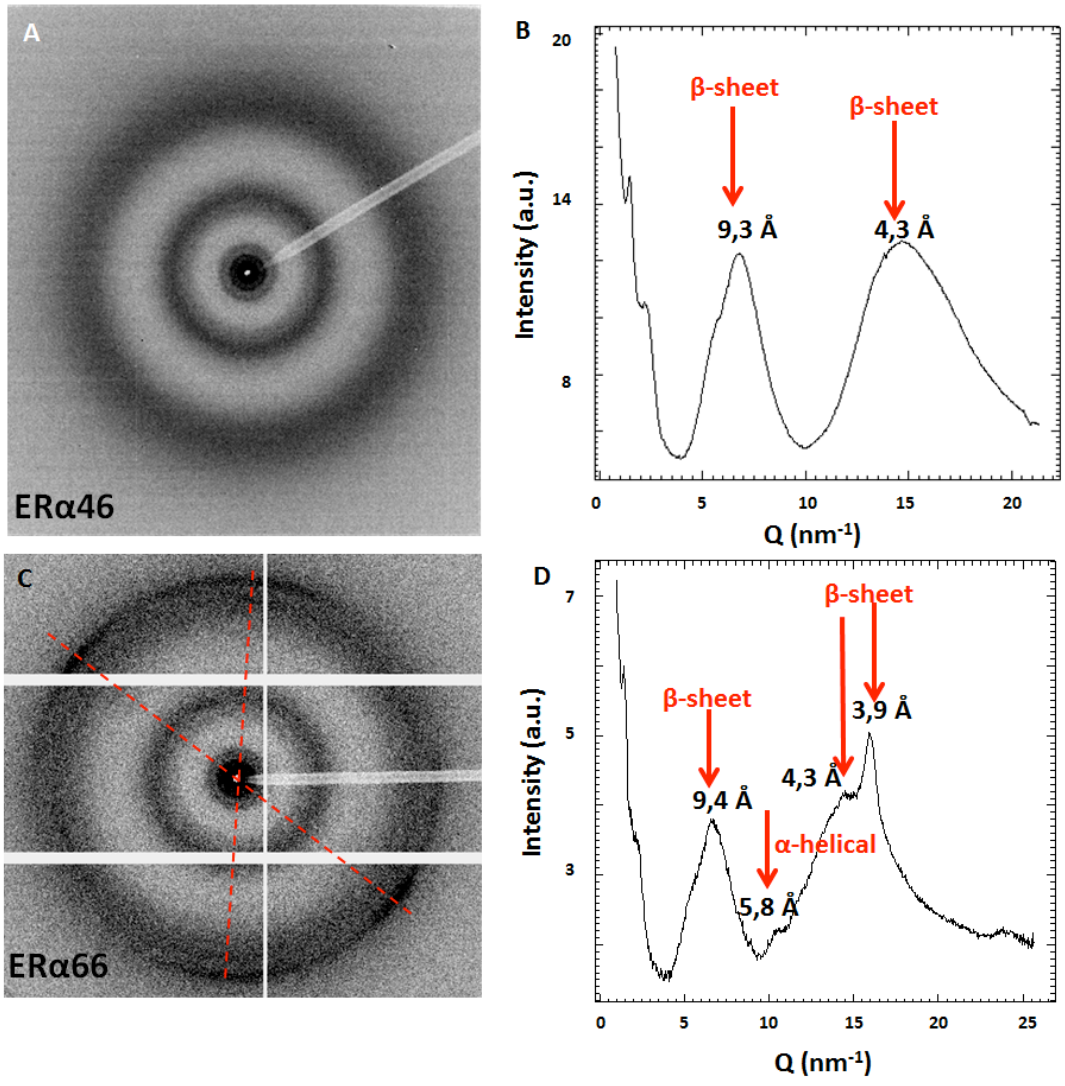

FIG. 5. A: typical XRD pattern coming from ERα46 sample; B: Azimuthal average of the XRD pattern in A (Q = 4πsin Θ/λ, where λ is the X-ray wavelength and Θ the diffraction angle); C: typical XRD pattern coming from ERα66 sample; D: B: Azimuthal average of the XRD pattern in C.

Finally, we characterized ERα samples dried on top of SU8 micropillars sitting on top of thin Si_3N_4 membranes by using the X-ray microdiffraction ID13 beamline at the European Synchrotron Radiation Facility. In figure 5A,B we plotted, respectively, a typical XRD pattern coming from ERα46 sample and its azimuthal averaging in terms of Q/I plots. The sample shows two evident d-spacings at 4.3 and 9.3 Å (related, respectively, to the distance between hydrogen bonded strands and to a β-sheet stacking) characteristic of a not oriented (isotropic) secondary β-sheet structure[22]. On the other hand, the ERα66 sample showed a quite evident anisotropy of the XRD patterns (Figure 5C) which was not shown by the patterns coming from ERα46. Indeed, it is possible to recognize a well-defined oriented quasi-crystalline cross β-sheet configuration (sharp peaks at 3.9 and 9.4 Å) contrasting the unoriented powder-like β-type material obtained in the ERα46 sample. The pattern indeed resembles a fiber-like one (the red dotted lines show the possible axes of two overlapping fiber structures) and the presence of the small peak at 5.8 Å (Figure 5D) may be attributed to the co-presence of a α-helical conformation[23], which is in nice accordance with the FTIR and Raman characterization results.

IV. SUMMARY AND CONCLUSIONS

In this work we showed how, by exploiting the superhydrophobic properties of SU8 micropillared surfaces, it is possible to obtain free-standing fibers coming from two biomedical relevant compounds, namely ERα46 and ERα66. The ability to grow the microstructured topology on different bulk substrates (i.e. CaF_2 windows and Si_3N_4 membranes) allowed to perform a multi-technique *in-situ* characterization by exploiting

Raman, FTIR and XRD techniques in absence of overlapping background signals. The achieved fibrillary morphology enhanced peculiar structural differences between the two estrogen receptors, whose presence is used as a biomarker in breast cancer prevention. In particular, the three performed characterizations seem to converge to the conclusion that, by a protein secondary structure point of view, while ERα46 features mainly β-sheet phases, ERα66 contains also some evident α-helical contributions which we attribute as a tentative hypothesis to the absence of the flexible A/B domain in ERα46[16]. The detection of discrimination factors in the Raman, FTIR and XRD signatures of these two proteins, could pave the basis for the development of a novel spectroscopic tool aiming at the structural identification of biomarkers linked to breast cancer disease. Further such approach can be an interesting alternative to more conventional methods employed to detect ERα46 and ERα66. Indeed, since no antibody presently available is able to recognize specifically ERα46 in immunohistochemistry (as all epitopes present in ERα66 are also theoretically present in ERα46), the only technique allowing the detection of ERα46 is Western blotting, a semi-quantitative, time–consuming and laborious technique which cannot be use routinely to perform diagnosis. In further works, we will improve the synthesis of the estrogen receptor samples in order to reach a higher crystalline phase of the dried samples in the context of sitting-drop crystallization experiments involving lotus-leaves-like engineered supports.

ACKNOWLEDGMENTS

We acknowledge the support of Christian Riekel and Martin Rosenthal at the ID13 beamline of the European Synchrotron Radiation Facility (ESRF) in Grenoble during the XRD measurements. The work at the INSERM unit 1048 is supported by INSERM, Université Toulouse III, and Faculté de Médecine Toulouse-Rangueil, Agence Nationale de la Recherche ANR N°-14-CE12-0021-01, Conseil Régional Midi-Pyrénées (R-BIO) and the Ligue Régionale contre le Cancer of the Comité de Haute-Garonne.

REFERENCES

[1] H. Cayron, B. Berteloite, C. Vieu, V. Paveau, J.-C. Cau and A. Cerf, Microelectron. Eng. **135**, 1-6 (2015).

[2] A. Lagraulet, J. Foncy, B. Berteloite, A. Esteve, M.-C. Blatche, L. Malaquin and C. Vieu, Nat. Meth. **12** (2015).

[3] E. Miele, A. Accardo, A. Falqui, M. Marini, A. Giugni, M. Leoncini, F. De Angelis, R. Krahne and E. Di Fabrizio, Small **11(1),** 134-140 (2015).

[4] J. Berthier, Microdrops and Digital Microfluidics. (William Andrew, 2008).

[5] J. Heikenfeld and M. Dhindsa, J. Adhes. Sci. Technol. **22**, 319–334 (2008).

[6] V. Hessel, H. Loewe, A. Mueller and G. Kolb, Chemical Micro Process Engineering. Wiley VCH GmbH, 2005.

[7] I.H. Chou, M. Benford, H.T. Beier, G.L. Coté, Nano Lett. **8(6),** 1729–1735 (2008).

[8] A. Keller, M. Fritzsche, Y.P. Yu, Q. Liu, Y.M. Li, M. Dong, F. Besenbacher, ACS Nano **5(4),** 2770–2778 (2011).

[9] A. Accardo, V. Shalabaeva, M. Cotte, M. Burghammer, R. Krahne, C. Riekel and S. Dante, Langmuir **30(11),** 3191–3198 (2014).

[10] A. Accardo, V. Shalabaeva, E. Di Cola, M. Burghammer, R. Krahne, C. Riekel and S. Dante, ACS Appl. Mater. Interfaces, **7(37),** 20875–20884 (2015).

[11] C. Neinhuis, and W. Barthlott, Ann. Bot. **79** 667–677 (1997).

[12] S.R. Johnston, Clin. Cancer Res. **16(7)**, 1979-87 (2010).

[13] G. Flouriot, H. Brand, S. Denger, R. Metivier, M. Kos, G. Reid, V. Sonntag-Buck and F. Gannon, Embo J. **19,** 4688-700 (2000).

[14] P. Barraille, P. Chinestra, F. Bayard and J.C. Faye, Biochem. Biophys. Res. Commun **257,** 84-8 (1999)

[15] G. Penot, C. Le Péron, Y. Mérot, E. Grimaud-Fanouillère, F. Ferrière, N. Boujrad, O. Kah, C. Saligaut, B. Ducouret, R. Métivier and G. Flouriot, Endocrinology **146(12),** 5474-84 (2005).

[16] G. Flouriot, H.Brand, B. Seraphin and F. Gannon, J. Biol. Chem. **277(29),** 26244-51 (2002).

[17] A. Accardo, E. Di Fabrizio, T. Limongi, G. Marinaro and C. Riekel, J. Synchrotron Radiat. **21(4),** 643-653 (2014).

[18] L. M. Miller, M. W. Bourassa and R.J. Smith, Biochim. Biophys. Acta **1828(10),** 2339-46 (2013).

[19] D. Naumann, Infrared Spectroscopy in Microbiology. In Encyclopedia of Analytical Chemistry; Meyers, R. A., Ed. (John Wiley & Sons Ltd., New York, 2000).

[20] N.C. Maiti, M.M. Apetri, M.G. Zagorski, P.R. Carey and V.E. Anderson, J. Am. Chem. Soc. **126,** 2399−2408 (2004).

[21] Z. Chi, X.G Chen, J.S. Holtz and S.A. Asher, Biochemistry **37(9),** 2854-64 (1998).

[22] R.N. Rambaran and L.C. Serpell, Prion **2,** 112−117 (2008).

[23] L.F. Drummy, D.M. Phillips, M.O. Stone, B.L. Farmer and R.R. Naik, Biomacromolecules **6(6),** 3328-33 (2005).